Polymer 51 (2010) 4408–4418

Contents lists available at ScienceDirect

Polymer

journal homepage: www.elsevier.com/locate/polymer

Comonomer-unit compositional distribution and its effect on thermal and crystallization behavior of bacterial poly(3-hydroxybutyrate-*co*-3-hydroxyhexanoate)

Fang Yu [a], Nobuo Nakamura [b], Yoshio Inoue [a,*]

[a] Department of Biomolecular Engineering, Tokyo Institute of Technology, Nagatsuta 4259-B-55, Midori-ku, Yokohama 226-8501, Japan
[b] GP Business Development Division, KANEKA Corporation, 5-1-1, Torikai-Nishi, Settsu, Osaka 566-0072, Japan

ARTICLE INFO

Article history:
Received 28 April 2010
Received in revised form
28 June 2010
Accepted 14 July 2010
Available online 23 July 2010

Keywords:
Polymer science
Polymer physics
Polymer materials

ABSTRACT

In order to clarify the relationships between comonomer-unit compositional distribution and physical properties of bacterial poly(3-hydroxybutyrate-*co*-3-hydroxyhexanoate) [P(3HB-*co*-3HHx)], the comonomer-unit composition and its distribution as well as their effects on the physical properties of P(3HB-*co*-3HHx) have been studied. A series of fractions with very different comonomer-unit composition but very narrow distribution were obtained by repeated fractionation and re-fractionation. It was found the as-bacterially synthesized P(3HB-*co*-3HHx) had very broad comonomer-unit compositional distribution. The solvent/non-solvent fractionation of P(3HB-*co*-3HHx) was found to be firstly regulated by the comonomer-unit composition and then by the molecular weight. Significant effect of the comonomer-unit compositional distribution on thermal and crystallization behavior as well as crystalline morphology of P(3HB-*co*-3HHx) was observed. It was concluded that as-bacterially synthesized P(3HB-*co*-3HHx) samples should be considered as polymer blends of component polymers with different 3HHx unit content, whose physical properties considerably depend on the comonomer-unit composition as well as comonomer-unit compositional distribution.

1. Introduction

The declining of globally available petroleum resources has urged great importance to look for the substitutes and solutions for petroleum oil-based polymeric materials. Hence, eco-friendly polymeric materials which can be produced by non-petroleum resources and biodegradable in nature are becoming one of the potential alternatives and being in increasing demands in nowadays society. Poly(hydroxyalkanoic acids) (PHAs) are one typical family of eco-friendly polymers, which can be produced by a wide variety of microorganisms and 100% biodegradable under the actions of various microorganisms and/or enzymes in nature [1–6]. So far, many efforts have been devoting on the basic scientific researches as well as the commercialization of PHAs with aiming to better serve the modern society [1–6].

Poly(3-hydroxybutyrate) [P(3HB)] is one of the widespread and well characterized members of PHA family [7]. However, its narrow processability window and relatively low impact resistance greatly confine its industrial applications [8–10] and studies on its copolymers, such as poly(3-hydroxybutyrate-*co*-3-hydroxyvalerate) [P(3HB-*co*-3HV)] [11–15], poly(3-hydroxybutyrate-*co*-3-hydroxypropionate) [P(3HB-*co*-3HP)] [16–20], poly(3-hydroxybutyrate-*co*-4-hyroxybutyrate) [P(3HB-*co*-4HB)] [21–23], and poly(3-hydroxybutyrate-*co*-3-hydroxyhexanoate) [P(3HB-*co*-3HHx)] [24–26] are expected as one of the solutions to improve the physical performance of P(3HB).

The success in biosynthesizing P(3HB-*co*-3HHx) was back up to 1993 [24], and since then more attentions have been paid on this completely bio-based polymer, as P(3HB-*co*-3HHx) possesses mechanical properties much superior to P(3HB) and very similar to one of the representative petroleum oil-based polymer, that is, low density polyethylene (LDPE) [27–29]. Full-scale development of P(3HB-*co*-3HHx) has already been piloted by Kaneka Corporation (Osaka, Japan). Wide application of P(3HB-*co*-3HHx) as one promising eco-friendly polymeric material in the near future is expected. Therefore, detail studies on the physical properties of P(3HB-*co*-3HHx) are desired in order to expand the industrial applications of P(3HB-*co*-3HHx).

Previous researches have featured bacterially synthesized PHA copolymers, such as P(3HB-*co*-3HV) [13,15], P(3HB-*co*-3HP) [16–20], P(3HB-*co*-4HB) [23] and P(3HB-*co*-3HHx) [28,29], as mixtures of

* Corresponding author. Tel.: +81 45 924 5794; fax: +81 45 924 5827.
E-mail address: inoue.y.af@m.titech.ac.jp (Y. Inoue).

0032-3861/$ – see front matter © 2010 Elsevier Ltd. All rights reserved.
doi:10.1016/j.polymer.2010.07.021

random copolymers with different comonomer-unit compositions, that is, these copolymers can be comonomer-unit compositionally fractionated through repeated processes of dissolution/precipitation by solvent/non-solvent mixed solvents, such as chloroform/*n*-heptane, acetone/water, or chloroform/acetone into a series of fractions with different comonomer-unit composition [30,31].

As one of the 3HB-containing copolymers, P(3HB-*co*-3HHx) is not an exception. Watanabe et al have reported that the as-bacterially synthesized P(3HB-*co*-3HHx) should be considered as natural polymer mixtures or blends of P(3HB-*co*-3HHx) with a broad comonomer-unit compositional distribution [28]. The thermal properties of P(3HB-*co*-3HHx) were reported to depend greatly on the comonomer-unit composition, as the positions and intensities of the DSC melting peaks of well-fractionated P(3HB-*co*-3HHx)s varied with 3HHx unit content and shifted to lower temperatures with increasing the 3HHx unit content [28]. Feng et al have conducted the fractionation at ambient temperature as well as the re-fractionation at 70 °C of P(3HB-*co*-3HHx)s with overall 3HHx unit content of 13.8, 18.0, 22.0 and 54.0 mol-% and they further demonstrated that all of the as-produced P(3HB-*co*-3HHx) samples were mixtures or blends of P(3HB-*co*-3HHx)s with different comonomer-unit compositions [29]. The fractionation of P(3HB-*co*-3HHx) was reported to mainly depend on the comonomer-unit composition, and when the comonomer-unit compositional distribution of P(3HB-*co*-3HHx) sample was narrow, the fractionation by molecular weight difference would become dominant [29]. Moreover, the effect of the comonomer-unit composition on thermal properties of well-fractionated P(3HB-*co*-3HHx) samples was further confirmed in a wide comonomer-unit composition range by Feng et al. [29].

However, it is found that the fractionated samples with similar comonomer-unit composition can still show different comonomer-unit compositional distribution, which exhibits significant effect on the physical properties of some bacterial PHAs [32]. So far, the effect of the comonomer-unit composition on thermal properties of P(3HB-*co*-3HHx) has been intensive while the effect of the comonomer-unit compositional distribution on physical properties of P(3HB-*co*-3HHx), such as thermal and crystallization behavior as well as crystalline morphology, has not been reported yet. In general, the fractionation is infeasible in industrial as it is not only laborious but also time-consuming. Therefore, it's essential to make a clear understanding of the effect of the comonomer-unit composition and its distribution on the physical performance of P(3HB-*co*-3HHx).

Table 1
Characterization of as-bacterially synthesized original P(3HB-*co*-7.5 mol-%3HHx) and its fractions.

Sample	Conc. Of *n*-heptane (vol.-%)	Amount of sample in fraction (wt.-%)	3HHx [b] (mol-%)	$M_n \times 10^5$	$M_w \times 10^5$	M_w/M_n
P(3HB-*co*-7.5 mol-%3HHx)[a]	–	100.0	7.5	1.5	3.4	2.3
Fraction 1	60.0	68.2	5.6	1.5	3.7	2.4
Fraction 2	61.5	3.8	8.0	2.0	4.1	2.0
Fraction 3	62.0	7.8	8.9	1.6	3.0	1.8
Fraction 4	62.5	2.2	10.0	1.2	2.5	2.1
Fraction 5	63.0	3.3	11.0	1.2	2.1	1.8
Fraction 6	63.5	1.2	10.4	0.9	1.8	2.1
Fraction 7	64.0	2.0	10.6	0.8	1.4	1.9
Fraction 8	65.0	1.3	11.5	0.7	1.3	1.9
Fraction 9	66.0	1.6	11.8	0.5	0.8	1.7
Fraction 10	67.5	1.0	12.3	0.3	0.6	1.7
Fraction 11	70.0	0.9	12.9	0.2	0.4	1.9
Fraction 12	75.5	0.5	12.7	–	–	–

[a] As-bacterially synthesized original sample.
[b] Measured by ^{1}H NMR.

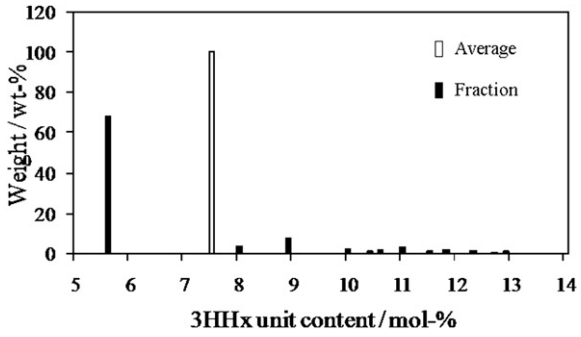

Fig. 1. Weight percent of fractions vs. 3HHx unit content for as-bacterially synthesized P(3HB-*co*-7.5 mol-%3HHx).

In this work, as-bacterially synthesized P(3HB-*co*-3HHx) samples with overall 3HHx unit content of 7.5, 11.2, 12.3 and 13.7 mol-% were used for analysis and a series of well-fractionated P(3HB-*co*-3HHx) samples with narrower and different comonomer-unit compositional distribution were obtained by repeated fractionation and re-fractionation. Subsequently, the thermal and crystallization behavior as well as the spherulite morphology were analyzed for P(3HB-*co*-3HHx) s with different comonomer-unit compositional distribution in order to investigate in detail the effect of the comonomer-unit compositional distribution on the physical properties of P(3HB-*co*-3HHx).

2. Experimental

2.1. Materials

A series of as-bacterially synthesized P(3HB-*co*-3HHx) samples with overall 3HHx unit content of 7.5, 11.2, 12.3 and 13.7 mol-% were kindly supplied by Kaneka Corporation (Osaka, Japan). The gene-recombinant bacterial strains based on *Ralstonia eutropha* PHB-4 pJRDdTc + 149NS171DG were used for the production of these P(3HB-*co*-3HHx) samples. The medium, the cultivation conditions and the procedures of purification of P(3HB-*co*-3HHx)s after cultivation were almost the same with those described in our previous reports [28,29].

Table 2
Characterization of the Fraction 1 of as-bacterially synthesized original P(3HB-*co*-7.5 mol-%3HHx) and its fractions.

Sample	Conc. Of *n*-heptane (vol.-%)	Amount of sample in fraction (wt.-%)	3HHx [b] (mol-%)	$M_n \times 10^5$	$M_w \times 10^5$	M_w/M_n
Fraction 1[a]	–	100.0	5.6	1.5	3.7	2.4
Re-fraction 1	58.0	87.4	5.5	1.4	3.6	2.5
Re-fraction 2	61.0 (After 1 day)[c]	6.0	7.7	1.6	3.9	2.5
Re-fraction 3	61.0 (After 3 days)[d]	3.0	8.2	1.0	2.5	2.5
Re-fraction 4	61.0 (After 10 days)[d]	2.4	8.7	1.1	2.1	1.9
Re-fraction 5	61.0 (After 27 days)[d]	0.9	9.8	0.7	1.9	2.9

[a] Fraction 1 of as-bacterially synthesized original P(3HB-*co*-7.5 mol-%3HHx).
[b] Measured by ^{1}H NMR.
[c] Indicating the waiting period from the addition of the current concentration of the non-solvent *n*-heptane to the collection of the current fraction.
[d] Indicating the waiting period from the collection of the previous fraction to the collection of the current fraction.

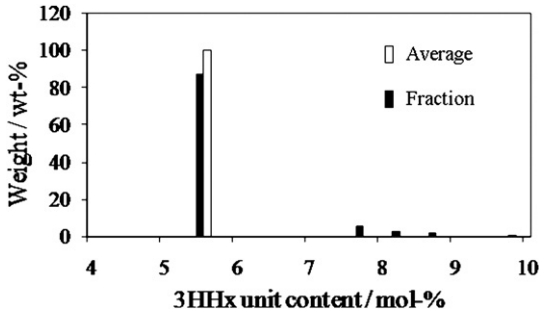

Fig. 2. Weight percent of Re-fractions vs. 3HHx unit content for Fraction 1 of as-bacterially synthesized P(3HB-*co*-7.5 mol-%3HHx).

Bacterially produced P(3HB) sample (M_n = 2.9 × 10^5, M_w = 6.5 × 10^5) was provided by PHB Industrial S/A (Brazil).

Before further measurement, all the samples were purified by precipitation in ethanol from the chloroform solution in order to remove any impurities.

2.2. Fractionation

The as-produced bacterial P(3HB-*co*-3HHx) sample was comonomer-unit compositionally fractionated with a chloroform/*n*-heptane mixed solvent at ambient temperature according to the procedures previously applied for the fractionation of P(3HB-*co*-3HV) and P(3HB-*co*-3HP) as described elsewhere [16,18,28,29]. The re-fractionation of once fractionated samples was conducted in the same way with taking careful consideration of the precipitation time. All the fractionation and re-fractionation processes were conducted at the same temperature of 20 °C.

Table 3
Characterization of the Re-fraction 1 of as-bacterially synthesized original P(3HB-*co*-7.5 mol-%3HHx) and its fractions.

Sample	Conc. of *n*-heptane (vol.-%)	Amount of sample in fraction (wt.-%)	3HHx[b] (mol-%)	$M_n \times 10^5$	$M_w \times 10^5$	M_w/M_n
Re-fraction 1[a]	–	100.0	5.5	1.4	3.6	2.5
Re'-fraction 1	52.0 (After 3 days)[c]	11.8	4.8	1.5	3.6	2.4
Re'-fraction 2	52.0 (After 3 days)[d]	6.3	4.8	1.4	3.9	2.7
Re'-fraction 3	52.0 (After 4 days)[d]	7.2	5.0	1.5	3.7	2.5
Re'-fraction 4	52.0 (After 3 days)[d]	4.5	5.2	1.6	3.6	2.2
Re'-fraction 5	52.0 (After 4 days)[d]	2.4	5.5	1.5	3.7	2.5
Re'-fraction 6	52.0 (After 3 days)[d]	4.5	5.2	1.4	3.6	2.5
Re'-fraction 7	54.0	22.8	5.5	1.4	3.8	2.6
Re'-fraction 8	56.5	29.4	6.1	1.2	3.4	2.8
Re'-fraction 9	59.0	5.3	7.3	1.3	3.1	2.3

[a] Re-Fraction 1 of as-bacterially synthesized original P(3HB-*co*-7.5 mol-%3HHx).
[b] Measured by ^{1}H NMR.
[c] Indicating the waiting period from the addition of the current concentration of the non-solvent *n*-heptane to the collection of the current fraction.
[d] Indicating the waiting period from the collection of the previous fraction to the collection of the current fraction.

2.3. Characterization of physical properties

2.3.1. Gel permeation chromatography (GPC)

Molecular weight of the samples was measured on TOSOH HLC-8220 GPC system (Tosoh Corporation, Tokyo, Japan) assembled with four TOSOH TSK GMH*2 + 2000 + 1000HXL columns and a VISCOTEK T-60AV viscometer. Chloroform was used as an eluent at a flowing rate of 1.0 ml/min. TOSOH TSK Standard polystyrene samples with narrow molecular distribution were used as standards to calibrate the GPC elution curve. The values of weight-average (M_w) and number-average (M_n) molecular weight were calculated through a VISCOTEK TriSEC Data Acquisition System.

2.3.2. Differential scanning calorimetry (DSC)

DSC measurements were carried out to monitor the melting behavior on a Pyris Diamond DSC instrument (PerkinElmer Japan Co., Ltd., Yokohama, Japan). The scales of temperature and heat flow at different heating rates were calibrated using an indium standard with nitrogen purging.

The DSC heating and cooling scanning procedures were conducted as follows. About 3–5 mg sample was encapsulated in an aluminum pan and was held at −50 °C for 2 min, and then heated to 180 °C at a heating rate of 10 °C min^{-1}. After holding for 2 min at 180 °C to allow complete melting, the sample was cooled to −50 °C at a constant cooling rate of −10 °C min^{-1}. Then, after holding at −50 °C for 2 min, the sample was reheated to 180 °C at 10 °C min^{-1}.

For isothermal crystallization analysis, about 3–5 mg sample capsulated in an aluminum pan was at first heated and held at 180 °C for 2 min and then quickly quenched to the isothermal crystallization temperature 90 °C at 100 °C min^{-1}. The sample was then reheated to 180 °C at a constant rate of 10 °C min^{-1} after the isothermal crystallization.

2.3.3. ^{1}H NMR spectroscopy

Solution 600 MHz ^{1}H NMR spectra were recorded on a Bruker Ultrashield 600 MHz/54 mm NMR spectrometer at room temperature. $CDCl_3$ and tetramethylsilane (TMS) were used as solvent and chemical shift reference, respectively. The assignments of the resonances in the ^{1}H NMR spectra were in accordance with those previously reported [25].

2.3.4. Polarized optical microscopy (POM)

The spherulite structure was characterized by POM with an Olympus BX50 polarized microscope (Olympus Co., Tokyo, Japan) equipped with a Mettler FP82HT hot stage device (Mettler-Toledo GmbH, Greifensee, Switzerland) and a FUJIX HC-2500 3CCD camera (Fujifilm Co., Tokyo, Japan). The film sample was sandwiched by two glass slides. After melting at 180 °C for 2 min, the sample was then quickly quenched to 90 °C for isothermal crystallization, and the formation of the spherulite morphology was observed.

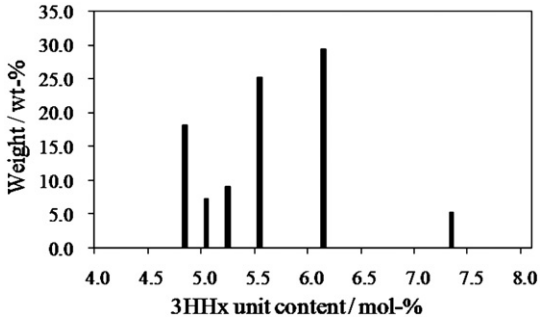

Fig. 3. Weight percent of Re'-fractions vs. 3HHx unit content for Re-Fraction 1 of Fraction 1 of as-bacterially synthesized P(3HB-*co*-7.5 mol-%3HHx).

3. Results and discussion

3.1. Fractionation

It is well known that the as-produced PHAs have a broad comonomer-unit compositional distribution and the fractionation of PHAs not only depends on the molecular weight but also on the comonomer-unit composition [28–31].

Table 1 shows the results of the fractionation of the as-bacterially synthesized P(3HB-*co*-3HHx) sample with overall 3HHx unit content of 7.5 mol-%, which is denoted as 'P(3HB-*co*-7.5 mol-% 3HHx)' in the following. The composition of the comonomer-unit in the copolymer was determined from the relative integrated intensities of the proton resonances of the 3HB and 3HHx repeating units in the ^{1}H NMR spectrum.

According to Table 1, P(3HB-*co*-7.5 mol-%3HHx) was fractionated into 12 fractions with the 3HHx unit content ranging from 5.6 to 12.9 mol-%. It is found that the fractionation is firstly depending on the comonomer-unit composition through to Fraction 5 that the 3HHx unit content increases with the fractionation proceeding. The molecular weight becomes the key factor regulating the later-stage of fractionation from Fractions 6 to 11 and it deceases with the fractionation proceeding. It indicates that both molecular weight and the comonomer-unit composition regulate the fractionation of P(3HB-*co*-3HHx), and the fractionation is firstly depending on the comonomer-unit composition and then the molecular weight becomes the dominant regulator.

To make a clear understanding of the comonomer-unit compositional distribution of P(3HB-*co*-7.5 mol-%3HHx), the weight composition of the fractions is plotted against the 3HHx unit content as shown in Fig. 1.

It is noticeable that the weight composition of the Fraction 1 is extraordinarily high. Almost similar phenomenon is often observed during the fractionation of P(3HB-*co*-3HHx) samples that a clear precipitation does not occur immediately after the addition of non-solvent *n*-heptane during the fractionation experiment, while after waiting for some period, lots of precipitation will appear, indicating a higher probability of inefficiency of the fractionation of some fractions. Accordingly, in order to further investigate the comonomer-unit compositional distribution of the first precipitated fraction, that is the Fraction 1 as shown in Table 1, the re-fractionation was conducted for this fraction and the results of the re-fractionation are shown in Table 2.

As shown in Table 2, the Fraction 1 with 3HHx unit content of 5.6 mol-% was refractionated into five fractions with the 3HHx unit content ranging from 5.5 to 9.8 mol-%. The 3HHx unit content increases with the fractionation proceeding from Re-fractions 1 to 5, and the molecular weight shows a slightly declining trend from Re-fractions 2 to 5. It indicates that the re-fractionation is generally regulated by the comonomer-unit composition. For Re-fractions 3–5, it is found that the precipitation of the fraction is induced only by waiting for a certain period without further addition of the non-solvent.

The comonomer-unit compositional distribution of Fraction 1 is shown in Fig. 2.

Similarly, a distinctly higher weight composition up to 87.4% is found for the Re-fraction 1, which is much higher than the other Re-fractions. Therefore, the re-fractionation for the second time, which is denoted as the re'-fractionation in the following, was conducted for the Re-fraction 1 by taking careful consideration of the precipitation period for the first fraction. The results of re'-fractionation are listed in Table 3 and the comonomer-unit compositional distribution of Re-fraction 1 is shown in Fig. 3.

It is shown in Table 3 that the Re-fraction 1 was refractionated into 10 re'-fractions with the 3HHx unit content ranging from 4.8 to 7.3 mol-% (Fig. 4). Similar to that revealed by Table 2, the Re'-fractions

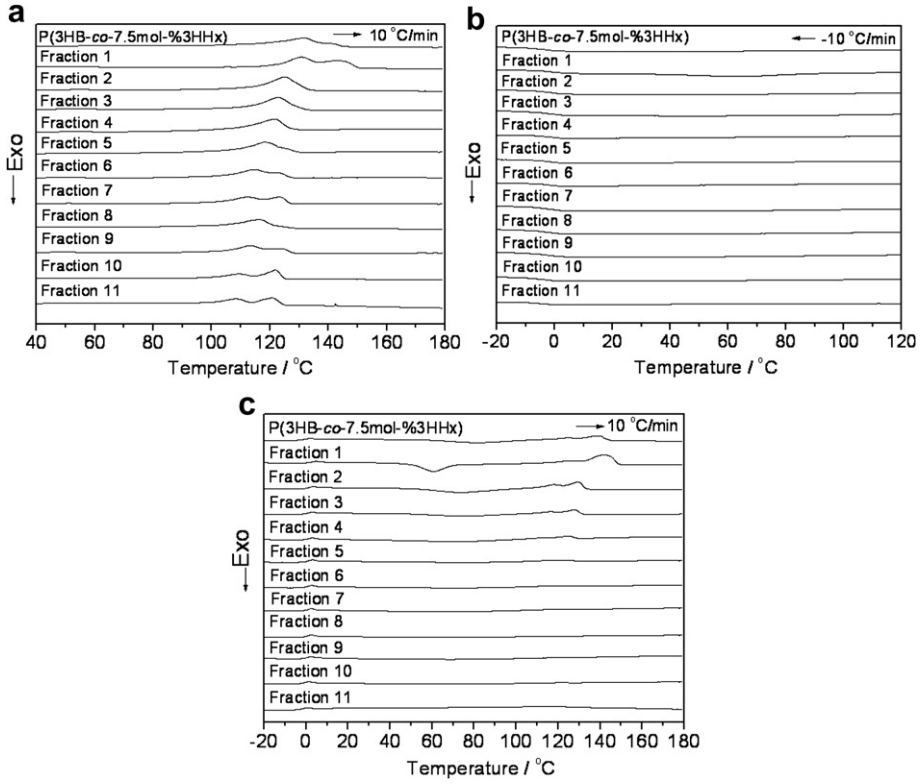

Fig. 4. DSC thermograms of (a) first heating (10 °C min^{-1}), then (b) cooling (10 °C min^{-1}), and (c) second heating (10 °C min^{-1}) scans of as-bacterially synthesized original P(3HB-*co*-7.5 mol-%3HHx) and its Fractions 1–11.

Table 4
Characterization of as-bacterially synthesized original P(3HB-*co*-11.2 mol-%3HHx), P(3HB-*co*-12.3 mol-%3HHx) and P(3HB-*co*-13.7 mol-%3HHx) as well as their fractions.

Sample	Conc. of *n*-heptane (vol.-%)	Amount of sample in fraction (wt.-%)	3HHx[b] (mol-%)	$M_n \times 10^5$	$M_w \times 10^5$	M_w/M_n
P(3HB-*co*-11.2 mol-%3HHx)[a]	–	100.0	11.2	0.9	2.6	2.9
Fraction 1	60.0	22.2	10.8	1.5	3.1	2.1
Fraction 2	61.0	5.0	8.4	1.9	3.9	2.1
Fraction 3	61.5	7.5	9.4	1.6	3.7	2.3
Fraction 4	62.0	12.5	10.2	1.6	2.9	1.8
Fraction 5	62.5	6.6	11.2	1.5	2.6	1.8
Fraction 6	63.0	8.8	12.2	1.3	2.3	1.7
Fraction 7	63.5	4.6	13.2	1.1	2.1	1.9
Fraction 8	64.0	4.0	14.2	1.0	1.8	1.8
Fraction 9	64.5	3.9	13.8	0.7	1.4	2.1
Fraction 10	65.0	2.3	15.5	0.8	1.5	2.0
Fraction 11	65.5	2.7	15.1	0.7	1.2	1.8
Fraction 12	66.0	1.4	16.3	0.8	1.1	1.5
Fraction 13	66.5	1.8	15.8	0.6	1.0	1.5
Fraction 14	67.0	1.8	15.2	0.4	0.7	1.8
Fraction 15	67.5	1.1	16.6	0.4	0.7	1.7
Fraction 16	68.0	0.6	18.1	0.5	0.7	1.5
Fraction 17	68.5	1.1	16.0	0.3	0.6	1.6
Fraction 18	69.5	1.3	17.4	0.3	0.5	1.5
Fraction 19	70.5	0.6	18.1	0.2	0.4	1.7
Fraction 20	72.0	1.1	16.8	0.2	0.3	1.5
Fraction 21	74.0	0.6	17.6	0.1	0.2	1.8
P(3HB-*co*-12.3 mol-%3HHx)[a]	–	100	12.3	0.6	2.2	3.7
Fraction 1	55.0	3.2	10.7	0.7	2.1	3.2
Fraction 2	55.0	2.5	8.1	0.5	1.6	3.1
Fraction 3	56.0	2.2	9.3	0.3	1.0	3.2
Fraction 4	56.5	2.9	9.2	0.3	0.8	2.5
Fraction 5	57.0	2.9	10.8	0.3	0.7	2.7
Fraction 6	58.0	4.5	9.2	0.2	0.7	3.0
Fraction 7	58.5	8.7	12.1	0.2	0.5	2.8
Fraction 8	60.0	18.7	9.8	0.2	0.5	2.5
Fraction 9	60.5	3.6	11.0	0.2	0.5	2.5
Fraction 10	61.5	8.9	11.7	0.2	0.4	2.1
Fraction 11	62.0	4.1	13.5	0.2	0.5	2.2
Fraction 12	62.5	6.0	12.8	0.2	0.3	1.8
Fraction 13	63.5	7.6	14.6	0.1	0.3	2.6
Fraction 14	64.0	1.3	18.1	0.2	0.3	1.9
Fraction 15	65.0	3.5	15.7	0.1	0.2	1.7
Fraction 16	66.0	1.8	20.2	0.1	0.2	1.7
Fraction 17	67.0	2.1	15.9	0.1	0.1	1.7
Fraction 18	69.0	2.2	19.5	–	–	–
P(3HB-*co*-13.7 mol-%3HHx)[a]	–	100	13.7	0.9	2.5	2.7
Fraction 1	60.0	12.9	8.1	1.5	3.7	2.4
Fraction 2	61.5	6.1	10.5	1.5	3.5	2.4
Fraction 3	62.0	9.1	10.4	1.9	3.4	1.8
Fraction 4	62.5	9.8	11.3	1.2	2.6	2.2
Fraction 5	63.0	6.8	12.4	1.1	2.3	2.1
Fraction 6	63.5	7.9	13.6	1.1	2.2	2.0
Fraction 7	64.0	5.1	14.9	1.0	2.1	2.2
Fraction 8	64.5	5.6	15.9	0.9	1.7	2.0
Fraction 9	65.0	4.3	15.6	0.8	1.3	1.7
Fraction 10	65.5	3.4	17.4	0.8	1.4	1.9
Fraction 11	66.0	3.7	17.4	0.5	1.2	2.3
Fraction 12	66.5	2.4	18.6	0.6	1.2	1.8
Fraction 13	67.0	2.1	18.6	0.5	0.9	1.9
Fraction 14	67.5	2.3	17.5	0.4	0.7	2.0
Fraction 15	68.0	1.6	20.3	0.4	0.8	2.2
Fraction 16	68.5	1.2	21.0	0.4	0.7	1.7
Fraction 17	69.0	1.5	19.4	0.3	0.6	1.8
Fraction 18	69.5	1.1	21.7	0.3	0.6	1.8
Fraction 19	70.5	1.4	21.1	0.2	0.5	1.9
Fraction 20	71.5	1.2	19.3	0.2	0.3	1.9
Fraction 21	72.5	0.6	21.5	0.2	0.3	1.8

[a] As-bacterially synthesized original sample.
[b] Measured by ^{1}H NMR.

1–5 were fractionated only by waiting for a certain period without further addition of the non-solvent *n*-heptane. The 3HHx unit content increases with the fractionation proceeding from Re'-fractions 1 to 5, and then the molecular weight becomes the main regulator and it decreases with the fractionation proceeding from Re'-Fractions 6 to 9.

According to above fractionation results that the concentration of the non-solvent *n*-heptane in the mixed solvent of the first fractionation is only 52% for the re'-fractionation, while 58 and 60% for those of the re-fractionation and the first fractionation, it indicates that the excessive non-solvent *n*-heptane in the mixed solvent is probably one of the causes for higher weight composition and broader comonomer-unit compositional distribution of the first fraction.

The interaction parameter is usually employed to detect the polymer–polymer interaction based on the Flory-Huggins theory [33]. It is considered that the interaction parameter is gradually adjusted when the solution separates from one homogenous phase into two phases during fractionation. After equilibrium between these two phases has been achieved, one phase can be separated and the interaction parameter is again readjusted in order to get new critical conditions of separation for other macromolecular species. In the case of the fractionation of PHA, as both the comonomer-unit composition and the molecular weight regulate the fractionation and the comonomer-unit composition is dominant at the beginning, a considerable period is required for the system to achieve equilibrium. With experimental experience of the fractionation of P(3HB-*co*-3HHx), this period is not counted by hours but by days. Usually it is difficult to handle during the practical experiment, which is suggested to consequently lead to the excessive addition of the non-solvent.

According to Tables 1–3, the comonomer-unit compositional distribution is from 5.6 to 12.9 mol-%, 5.5 to 9.8 mol-% and 4.8 to 7.3 mol-% for the first fractionation, re-fractionation and re'-fractionation, respectively. It indicates that the comonomer-unit compositional distribution becomes narrower and narrower by fractionation and the repeated fractionation is one of the better methods to obtain sample with a narrow comonomer-unit compositional distribution.

In order to find a regulation principle for the fractionation of P(3HB-*co*-3HHx), the fractionation was also conducted on the as-bacterially synthesized P(3HB-*co*-3HHx) samples with overall 3HHx unit content of 11.2, 12.3 and 13.7 mol-%, which are hereafter denoted as P(3HB-*co*-11.2 mol-%3HHx), P(3HB-*co*-12.3 mol-% 3HHx) and P(3HB-*co*-13.7 mol-%3HHx), respectively. The fractionation results are summarized in Table 4.

According to the Table 4, the ranges of the comonomer-unit compositional distribution are 8.4–18.1 mol-%, 8.1–20.2 mol-% and

Table 5
Thermal data of the as-bacterially synthesized original P(3HB-*co*-7.5 mol-%3HHx) and its fractions 1–11.

Sample	3HHx/%	T_g[a]/°C	T_m[b]/°C	ΔH_m[b]/J g^{-1}	Crystallinity[c]/%
P(3HB-*co*-7.5 mol-%3HHx)	7.5	−2.4	131.6	56.5	38.5
Fraction 1	5.6	1.0	130.8	65.4	44.6
Fraction 2	8.0	−0.3	125.1	57.5	39.2
Fraction 3	8.9	−0.6	122.7	51.8	35.3
Fraction 4	10.0	−1.1	121.6	42.8	29.2
Fraction 5	11.0	−0.6	118.7	48.6	33.2
Fraction 6	10.4	−1.2	114.9	40.0	27.3
Fraction 7	10.6	−1.1	112.1	38.9	26.5
Fraction 8	11.5	−1.4	116.2	45.1	30.8
Fraction 9	11.8	−1.3	113.4	33.3	22.7
Fraction 10	12.3	−2.7	109.3	33.9	23.1
Fraction 11	12.9	−3.4	108.2	42.7	29.1

[a] Measured by the second heating scan DSC diagram (10 °C min^{-1}).
[b] Measured by the first heating scan DSC diagram (10 °C min^{-1}). For thermograms with dual melting peaks, Tm was taken as the top of lower temperature peak.
[c] Calculated by assuming the thermodynamic melting enthalpy per gram of completely crystalline P(3HB) to be 146.6 J g^{-1}.

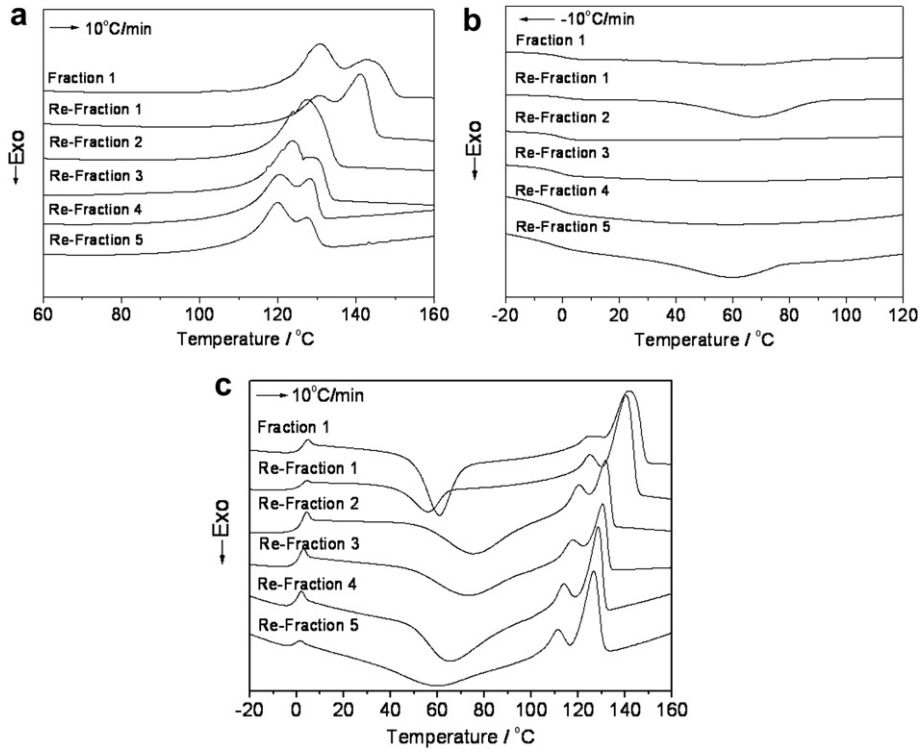

Fig. 5. DSC thermograms of (a) first heating (10 °C min^{-1}), then (b) cooling (10 °C min^{-1}), and (c) second heating (10 °C min^{-1}) scans of Fraction 1 and its Re-fractions 1–5.

8.1–21.7 mol-% for P(3HB-*co*-11.2 mol-%3HHx), P(3HB-*co*-12.3 mol-% 3HHx) and P(3HB-*co*-13.7 mol-%3HHx), respectively. The 3HHx unit contents of the first fractions of P(3HB-*co*-11.2 mol-%3HHx) and P(3HB-*co*-12.3 mol-%3HHx) are both significantly higher than the following fractions, indicating a higher probability of inefficiency in the fractionation of these first fractions. For the fractionation of P(3HB-*co*-11.2 mol-%3HHx), the 3HHx unit content increases with the fractionation proceeding from Fractions 2 to 8, and the molecular weight decreases from Fractions 10 to 21. For the fractionation of P(3HB-*co*-12.3 mol-%3HHx), the 3HHx unit content increases with the fractionation proceeding from Fractions 2 to 5, and the molecular weight decreases from Fractions 6 to 17. Similarly for the fractionation of P(3HB-*co*-13.7 mol-%3HHx), the 3HHx unit content increases from Fractions 1 to 8, and the molecular weight decreases from Fractions 11 to 21. It confirms a principle that both molecular weight and the comonomer-unit composition regulate the efficiency of the fractionation of P(3HB-*co*-3HHx), and the fractionation firstly depends on the comonomer-unit composition and then the molecular weight becomes the dominant regulator. These results also further demonstrate that the as-bacterially synthesized P(3HB-*co*-3HHx) has a very broad comonomer-unit compositional distribution.

Table 6
Thermal data of Fraction 1 of as-bacterially synthesized original P(3HB-*co*-7.5 mol-% 3HHx) and its Re-fractions 1 to 5.

Sample	3HHx/%	T_g[a]/°C	T_m[b]/°C	ΔH_m[b]/J g^{-1}	Crystallinity[c]/%
Fraction 1[d]	5.6	1.0	130.8	65.4	44.6
Re-fraction 1	5.5	0.9	130.1	69.3	47.3
Re-fraction 2	7.7	0.5	127.6	65.3	44.5
Re-fraction 3	8.2	−0.9	123.7	61.6	42.0
Re-fraction 4	8.7	−1.5	120.3	35.8	24.4
Re-fraction 5	9.8	−0.8	119.9	38.6	26.3

[a] Measured by the second heating scan DSC diagram (10 °C min^{-1}).
[b] Measured by the first heating scan DSC diagram (10 °C min^{-1}). For thermograms with dual melting peaks, Tm was taken as the top of lower temperature peak.
[c] Calculated by assuming the thermodynamic melting enthalpy per gram of completely crystalline P(3HB) to be 146.6 J g^{-1}.
[d] Fraction 1 of as-bacterially synthesized original P(3HB-*co*-7.5 mol-%3HHx).

3.2. Thermal and crystallization behavior

In order to investigate the effect of comonomer-unit composition and its distribution on physical properties of P(3HB-*co*-3HHx), the thermal and crystallization properties were investigated for unfractionated original P(3HB-*co*-7.5 mol-%3HHx) and a series of its fractions and re-fractions with different comonomer-unit composition and distribution.

The DSC diagrams of the first heating, then cooling and second heating scans of as-bacterially synthesized P(3HB-*co*-7.5 mol-% 3HHx) and its fractions are shown in Fig. 4(a)–(c). The thermal data are summarized in Table 5.

It is shown in Table 5 that the melting points, heat of fusion and the crystallinity of the original sample P(3HB-*co*-7.5 mol-%3HHx) are all lower or higher than those of its fractions, indicating the blend nature of the original sample. The melting points, heat of fusion and the crystallinity of the Fractions 1–5 generally decrease with increasing the 3HHx unit content, indicating a clear effect of the comonomer-unit composition on the thermal behavior of the fractionated P(3HB-*co*-3HHx). While for Fractions 6–11, the regulational effect of comonomer-unit composition on the melting points, heat of fusion and the crystallinity is less obvious. According to the fractionation results, the fractionation firstly depends on the comonomer-unit composition and then is regulated by the molecular weight. It is considered that, though there is a higher possibility for the first fraction, Fraction 1, to still bear a broader comonomer-unit compositional distribution, the Fractions 1–5 have relatively narrower comonomer-unit compositional distribution compared to Fractions 6–11, as the fractionation for the former fractions is regulated by the comonomer-unit composition, while that for the later fractions is regulated by molecular weight. Therefore, the comonomer-unit composition does not clearly regulate the thermal

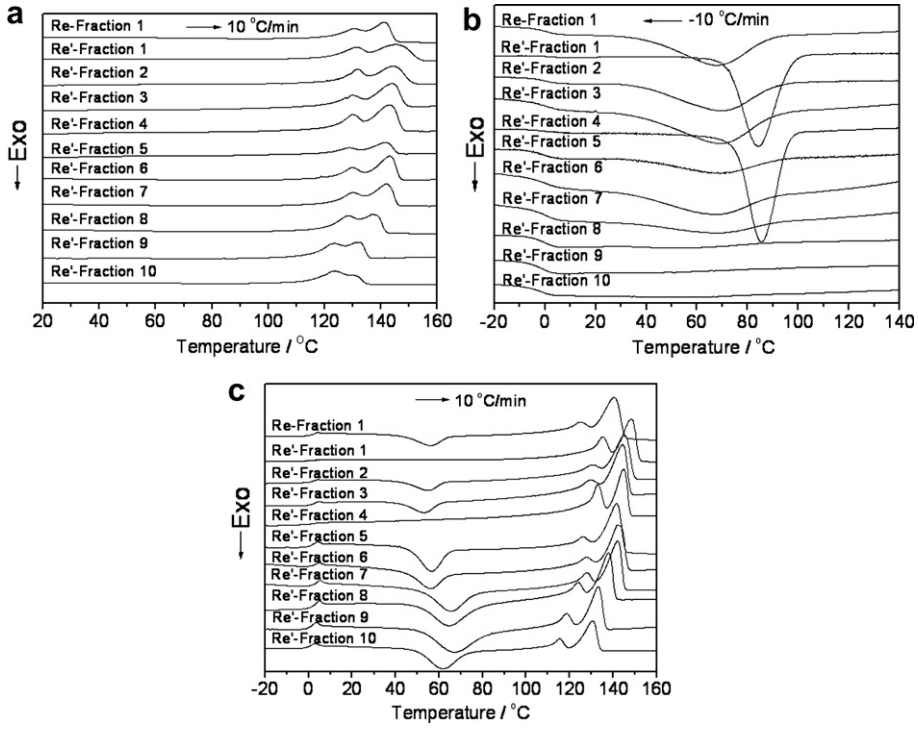

Fig. 6. DSC thermograms of (a) first heating (10 °C min^{-1}), then (b) cooling (10 °C min^{-1}), and (c) second heating (10 °C min^{-1}) of Re-Fraction 1 and its Re'-Fractions 1–10.

properties of Fractions 6–11, because their comonomer-unit compositional distribution may not be compositionally narrow. According to Fig. 4(a)–(c), a melt crystallization peak during the cooling process and a cold crystallization peak during the second heating process are observed for Fraction 1. Fraction 2, however, only shows a very broad cold crystallization peak during the second heating process. For the rest of the fractions, almost no crystallization peak can be observed during the thermal procedure, indicating a very slow crystallization behavior of these fractions. The difference in the crystallization of these fractions is considered to be caused by both the comonomer-unit composition and its distribution. As for Fraction 1, it could be refractionated into 5 fractions with 3HHx unit content ranging from 5.5 to 9.8 mol-%, and its refraction, Re-Fraction 1 could further be refractionated into 10 fractions with 3HHx unit content ranging from 4.8 to 7.3 mol-%, as shown in Tables 2 and 3, it is suggested that the faster crystallization of Fraction 1 is ascribed to its mixed fractions with lower 3HHx unit content.

The DSC diagrams of the first heating, then cooling and the second heating scans of Fraction 1 and its re-fractions are shown respectively in Fig. 5(a)–(c) and the thermal data are summarized in Table 6.

According to Fig. 5, the double melting points are observed for almost all samples during the first heating process, and cold crystallization peaks can be observed for Re-fractions 1 and 5 during the cooling process, moreover melt crystallization peaks can be observed for all samples during the second heating process. It indicates that the crystallization rate of Re-fractions 1 and 5 is faster, probably because Re-Fraction 1 still has a broad comonomer-unit compositional distribution and Re-fraction 5 has a relatively smaller molecular weight. The melting points, the heat of fusion and the crystallinity of the Fractions 1–5 shown in Table 6 generally decrease with increasing the 3HHx unit content. According to the fractionation result, the fractionation of Re-fractions 1–5 is regulated by the comonomer-unit composition. It confirms that the comonomer-unit composition exhibits a clear regulational effect on the thermal behavior of fractionated P(3HB-*co*-3HHx) when the fractionation of these fractions is regulated by the comonomer-unit composition.

The DSC diagrams of the first heating, then cooling and the second heating scans of Re-Fraction 1 and its re'-fractions are shown respectively in Fig. 6(a)–(c) and the thermal data are summarized in Table 7.

According to Fig. 6, the double melting peaks are observed for all samples during the first heating process, and cold crystallization peaks can be observed for almost all samples during the cold crystallization process, in particular, a very sharp cold crystallization peak is observed for Re'-Fractions 1 and 4, while no melt crystallization peaks can be observed for these two Re-fractions during second heating process. It indicates that Re'-Fractions 1 and 4 have very fast crystallization rate, which is suggested to be caused

Table 7
Thermal data of Re-Fraction 1 of as-bacterially synthesized original P(3HB-*co*-7.5 mol-%3HHx) and its Re'-Fractions 1–10.

Sample	3HHx/%	T_g[a]/°C	T_{m1}[b]/°C	ΔH_m[b]/J g^{-1}	Crystallinity[c]/%
Re-fraction 1[d]	5.5	0.9	130.1	69.3	47.3
Re'-fraction 1	4.8	0.7	131.2	76.3	52.0
Re'-fraction 2	4.8	1.1	131.6	72.9	49.7
Re'-fraction 3	5.0	2.1	129.6	71.5	48.8
Re'-fraction 4	5.2	1.7	130.0	73.5	50.1
Re'-fraction 5	5.5	0.7	128.7	70.6	48.2
Re'-fraction 6	5.2	1.6	129.5	62.7	42.8
Re'-fraction 7	5.5	1.7	129.7	67.4	46.0
Re'-fraction 8	6.1	1.3	128.5	72.1	49.2
Re'-fraction 9	7.3	−0.6	123.5	51.7	35.3
Re'-fraction 10	8.5	−0.9	123.7	41.3	28.2

[a] Measured by the second heating scan DSC diagram (10 °C min^{-1}).
[b] Measured by the first heating scan DSC diagram (10 °C min^{-1}). For thermograms with dual melting peaks, Tm was taken as the top of lower temperature peak.
[c] Calculated by assuming the thermodynamic melting enthalpy per gram of completely crystalline P(3HB) to be 146.6 J g^{-1}.
[d] Re-Fraction 1 of as-bacterially synthesized original P(3HB-*co*-7.5 mol-%3HHx).

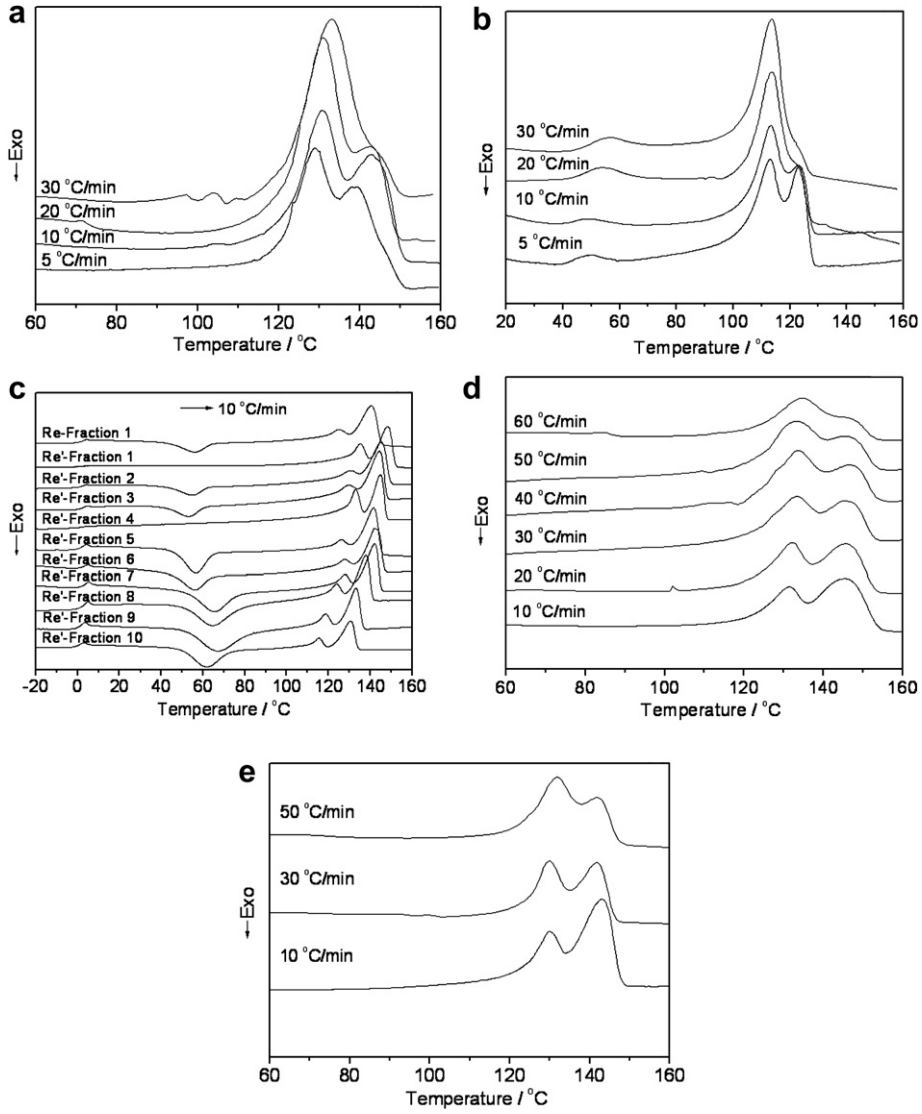

Fig. 7. DSC thermograms of first heating at different heating rates for (a) Fraction 1, (b) Fraction 9, (c) Re-Fraction 1, (d) Re'-Fraction 1 and (e) Re'-Fraction 4.

by a higher sequence order of the 3HB unit in their polymer chains and it will be discussed in details in the checking of the double melting peaks section. Similarly, the 3HHx unit content as shown in Table 7 clearly regulates the thermal behavior of Re'-Fractions 1–5, while its regulational effect on the thermal behavior of Re'-Fractions 6–10 is less obvious. According to the fractionation results, it again confirms that the comonomer-unit composition shows a clear regulational effect on the thermal behavior of fractionated P(3HB-*co*-3HHx) when the fractionation of these fractions is regulated by the comonomer-unit composition, while the regulation is less obvious when the fractionation is regulated by the molecular weight.

According to the data shown in Table 7, the comonomer-unit composition of the original Re-Fraction 1 sample is the same as those of two of its re'-fractions, that is, Re'-Fractions 5 and 7, while the melting point, the heat of fusion and the crystallinity are different with each other. The difference in thermal properties between the original sample and its fractions is considered to be caused by comonomer-unit compositional distribution as the original Re-Fraction 1 sample obviously has a broader comonomer-unit compositional distribution than those of Re'-Fractions 5 and 7. As the reason for the difference in thermal properties between Re'-Fractions 5 and 7, it's also considered to be caused by the comonomer-unit compositional distribution, because the fractionation of Re'-Fractions 5 is regulated by the comonomer-unit composition, while that of Re'-Fractions 7 is regulated by the molecular weight, according to the fractionation results, indicating that these two re'-fractions have different comonomer-unit compositional distribution.

According to Fig. 6(a)–(c), an obvious difference in thermal behavior between Re'-Fractions 1 and 2, which have the same 3HHx unit content of 4.8 mol-%, are observed. A sharp crystallization peak is observed for Re'-Fraction 1 during the cooling, and the crystallization finishes almost completely during the cooling process. Moreover, no cold crystallization peak can be observed during the second heating. The Re'-Fraction 2, however, shows a broad crystallization peak during the cooling process and a cold crystallization peak during the second heating. The crystallinity of Re'-Fraction 1 is significantly higher than that of Re'-Fraction 2. The similar difference in thermal behavior is also observed for another pair of re'-fractions, that is, the Re'-Fraction 4 and Re'-Fraction 6, which also have the same 3HHx unit content of 5.2 mol-%. It is

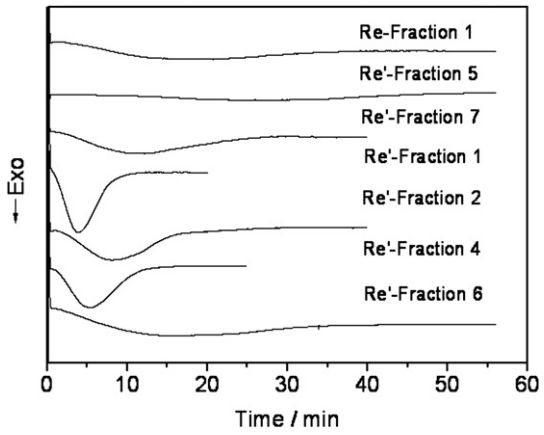

Fig. 8. Heat flow vs. time curves during isothermal crystallization at 90 °C for Re-Fraction 1, Re'-Fractions 1, 2, 4, 5, 6 and 7.

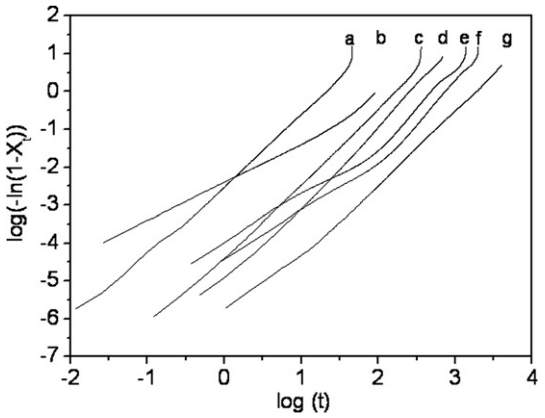

Fig. 9. Avrami plots at crystallization temperature of 90 °C for (a) Re-Fraction 1, (b) Re'-Fraction 5, (c) Re'-Fraction 7, (d) Re'-Fraction 1, (e) Re'-Fraction 2, (f) Re'-Fraction 4 and (g) Re'-Fraction 6.

suggested to be caused by the different comonomer-unit compositional distribution. In the case of Re'-Fractions 1 and 2, as the first fraction, Re'-Fraction 1 has a higher possibility to bear a relatively broader comonomer-unit compositional distribution than that of Re'-Fraction 2, according to the analysis on the fractionation. In the case of Re'-Fractions 4 and 6, the fractionation of Re'-Fraction 4 is regulated by the comonomer-unit composition, while that of the Re'-Fraction 6 is regulated by the molecular weight.

The double melting peaks during DSC first heating scan were observed for Fractions 1, 5–7, 9–11, Re-fractions 1, 3–5 and the Re'-Fractions 1–11 of the as-produced original P(3HB-*co*-7.5 mol-% 3HHx). In order to know whether one of these peaks is caused by recrystallization, DSC measurements at different heating rates were carried out for the Re'-Fractions 1 and 4, as well as Fractions 1 and 9, Re-Fraction 1. The results are shown in Fig. 7(a)–(e).

It shows obviously that both the position and the intensity of the higher temperature-side peak vary with the heating rate, in contrast to the peak appearing at lower temperature-side for Fractions 1 and 9, as well as Re-Fraction 1, indicating that the lower temperature-side peak is a real melting peak of the crystal formed originally, while that at higher temperature-side is the melting peak of the crystal formed by recrystallization during the DSC heating process. This result is in agreement with that previously reported [28]. While for Re'-Fractions 1 and 4, though the position and intensity of the higher temperature-side peak vary with the heating rate, the changes appear less obvious compared to Fractions 1 and 9, as well as Re-Fraction 1, as seen in Fig. 7(d) and (e). There are three reasons considered for this phenomenon. First, it is known that the P(3HB-*co*-3HHx) with lower 3HHx unit content has the P(3HB)-homopolymer type crystalline lattice [34]. The second is both Re'-Fraction 1 and Re'-Fraction 4 have very low 3HHx unit content of 4.8 and 5.2, respectively, according to Table 3, and the third reason is both of these two samples have very narrower comonomer-unit compositional distribution according to the fractionation results. These three reasons are suggested to contribute to a higher sequence order of the 3HB unit in the polymer chains leading to a quick rearrangement into the crystals with better packing during heating process.

Therefore, it can be concluded that both the comonomer-unit composition and its distribution show significant effect on the thermal behavior of P(3HB-*co*-3HHx).

To investigate the effect of the comonomer-unit compositional distribution on the crystallization behavior, the isothermal crystallization was analyzed for the samples with similar comonomer-unit composition while different comonomer-unit compositional distribution. Fig. 8 shows the plot of heat flow against time during isothermal crystallization at 90 °C for 1 h for the original sample Re-Fraction 1, and the Re'-Fractions 1, 2, 4, 5, 6 and 7.

Avrami equation [35], which is expressed as:

$$1 - X_t = \exp(-kt^n)$$

is applied to analyze the isothermal crystallization kinetics. The equation can also be rewritten as:

$$\log[-\ln(1 - X_t)] = \log k + n\log t$$

where X_t, k, n, and t are mass fraction crystallinity, rate constant, Avrami exponent, and time of crystallization, respectively. Both k and n depend on the mechanism of the nucleation as well as the growth geometry. The crystallization half time ($t_{1/2}$) is obtained from:

$$t_{1/2} = (\ln 2/k)^{1/n}$$

Plots of log [$-\ln(1 - X_t)$] against log t are shown in Fig. 9. From this plot, the values of n and k together with that of $t_{1/2}$ are estimated and the results are listed in Table 8.

According to Table 8, the n value of the investigated samples except the Re'-Fraction 5 is around 2, indicating the similar nucleation mechanisms of these samples isothermally crystallized at 90 °C. It's known that the n value is dependent on crystal geometry, nucleation mode (athermal or thermal) and rate determination step (contact or diffusion) [36]. In general, the athermal nucleation is the nuclei growth depends on external conditions, such as temperature, pressure etc., while the thermal nucleation is the nuclei grow through the thermally activated process [36]. The relatively lower n value (1.57) of the Re'-Fraction 5 is probably because it shows a crystallization mechanism of spherical growth

Table 8
Values of n, k, $t_{1/2}$ of Re-Fraction 1 of as-bacterially synthesized original P(3HB-*co*-7.5 mol-%3HHx), Re'-Fractions 1, 2, 4, 5, 6 and 7 for isothermal crystallizing at 90 °C.

Sample	3HHx/mol-%	n	k	$t_{1/2}$/min
Re-fraction 1	5.5	1.96	2.0×10^{-6}	11.3
Re'-fraction 5	5.5	1.57	8.5×10^{-6}	22.7
Re'-fraction 7	5.5	2.07	1.5×10^{-6}	9.0
Re'-fraction 1	4.8	2.18	5.3×10^{-6}	3.7
Re'-fraction 2	4.8	1.86	5.4×10^{-6}	9.2
Re'-fraction 4	5.2	2.04	5.2×10^{-6}	5.4
Re'-fraction 6	5.2	1.97	1.7×10^{-6}	11.6

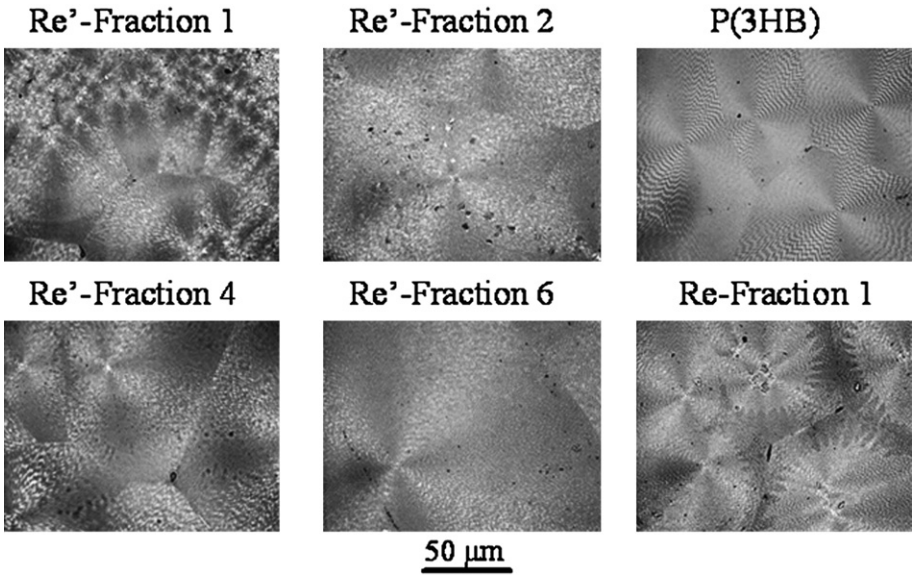

Fig. 10. Spherulite morphology observed by POM at the crystallization temperature 90 °C for Re'-Fractions 1, 2, 4 and 6, P(3HB) and Re-Fraction 1, scale bar for all: 50 μm.

in diffusion step from athermal (simultaneous) [36]. The $t_{1/2}$ of the original sample Re-Fraction 1 and Re'-Fractions 5 and 7 are 11.3, 22.7 and 9.0 min, respectively, indicating the different crystallization behavior among these samples which have the same comonomer-unit composition. For Re'-Fractions 1 and 2, though with the similar comonomer-unit composition, the $t_{1/2}$ of the Re'-Fraction 2 (9.2 min) is distinctly longer than that of the Re'-Fraction 1 (3.7 min). The similar result is also observed for another pairs, that is, the $t_{1/2}$ of the Re'-Fraction 6 is 11.6 min which is distinctly longer than its counterpart Re'-Fraction 4 of 5.4 min. This result further confirms that the comonomer-unit compositional distribution exhibits significant effect on the crystallization behavior of P(3HB-*co*-3HHx).

3.3. Spherulite morphology

The spherulite morphology was observed at 90 °C for the Re'-Fractions 1, 2, 4 and 6, as well as for P(3HB) and the Re-Fraction 1 to make a comparison. All the spherulites are developed under the same conditions (first melt at 180 °C for 2 min, then quickly quenched from the melt to 90 °C, and then isothermally crystallized). The results are shown in Fig. 10.

It is shown clearly that the original sample Re-Fraction 1 and its re'-fractions Re'-Fractions 1, 2, 4 and 6 show the spherulite morphology similar to that of P(3HB), while the number and the size of the spherulite are different. The spherulite size of Re-Fraction 1 is larger than that of Re'-Fraction 1, while it is smaller than those of Re'-Fractions 2, 4 and 6. On the other hand, the number of the spherulite of Re-Fraction 1 is less than that of Re'-Fraction 1, while more than those of Re'-Fractions 2, 4 and 6, indicating the blend nature of the original sample Re-Fraction 1. Though with the same comonomer-unit composition, the spherulite size of Re'-Fractions 1 and 4 is relatively smaller, while the number of the spherulite is relatively more than those of the respective counterparts, Re'-Fractions 2 and 6, indicating faster crystallization of Re'-Fractions 1 and 4. It is considered to be caused by higher sequence order of the 3HB unit in the polymer chains of Re'-Fractions 1 and 4 as discussed in the checking of the double melting peaks section. This result is in accordance with that of the investigation based on DSC and it further confirms that the comonomer-unit compositional distribution also exhibits a significant effect on the crystalline morphology.

4. Conclusion

The comonomer-unit compositional distribution of P(3HB-*co*-3HHx) was discussed in details based on the solvent/non-solvent fractionation of four as-bacterially synthesized P(3HB-*co*-3HHx) samples with overall 3HHx unit content of 7.5, 11.2, 12.3 and 13.7 mol-%. It is further confirmed that the as-bacterially synthesized P(3HB-*co*-3HHx) has a very broad comonomer-unit compositional distribution. Besides, with the combination of DSC and POM analysis, it is revealed that the comonomer-unit compositional distribution exhibits significant effect on the thermal and crystallization behavior as well as the crystalline morphology of P(3HB-*co*-3HHx). Accordingly, the comonomer-unit compositional distribution should be considered as one of the important factors regulating the physical performance of P(3HB-*co*-3HHx). Therefore, both the comonomer-unit composition and comonomer-unit compositional distribution should be carefully taken into consideration during the study on the structure–properties relationship, industrial processing and polymer blending of P(3HB-*co*-3HHx).

References

[1] Lee SY, Chang HN. Adv Biochem Eng Biotechnol 1995;52:27–58.
[2] Steinbüchel A, Valentin HE. FEMS Microbiol Lett 1995;128:219–28.
[3] Sudesh K, Abe H, Doi Y. Prog Polym Sci 2000;25:1503–55.
[4] Steinbüchel A. Curr Opin Biotechnol 1992;3:291–7.
[5] Steinbüchel A, Füchtenbusch B. Trends Biotechnol 1998;16:419–27.
[6] Anderson AJ, Dawes EA. Microbiol Rev 1990;54:450–72.
[7] Lemoigne M. Bull Soc Chim Biol 1926;8:770–82.
[8] Howells ER. Chem Ind 1982;8:508–11.
[9] King PP. Chem Technol Biotechnol 1982;32:2–8.
[10] Holmes PA. Phys Technol 1985;16:32–6.
[11] Bloembergen S, Holden DA, Hamer GK, Bluhm TL, Marchessault RL. Macromolecules 1986;19:2865–71.
[12] Kunioka N, Tamaki A, Doi Y. Macromolecules 1989;22:694–7.
[13] Kamiya N, Yamamoto Y, Inoue Y, Chûjô R. Macromolecules 1989;22:1676–82.
[14] Doi Y, Kunioka M, Nakamura Y, Soga K. Macromolecules 1986;19:2860–4.
[15] Yoshie N, Menju H, Sato H, Inoue Y. Macromolecules 1995;28:6516–21.
[16] Cao A, Ichikawa M, Kasuya K, Yoshie N, Asakawa N, Inoue Y, et al. Polym J 1996;28:1096–102.
[17] Cao A, Kasuya K, Abe H, Doi Y, Inoue Y. Polymer 1998;39:4801–16.
[18] Arai Y, Cao A, Yoshie N, Inoue Y. Polym Int 1999;48:1219–28.
[19] Wang Y, Ichikawa M, Cao A, Yoshie N, Inoue Y. Macromol Chem Phys 1999;200:1047–53.
[20] Cao A, Asakawa N, Yoshie N, Inoue Y. Polymer 1999;40:3309–22.
[21] Doi Y, Segawa A, Kunioka M. Int J Biol Macromol 1990;12:106–11.

[22] Saito Y, Doi Y. Int J Biol Macromol 1994;16:99–104.
[23] Shi F, Ashby RD, Gross RA. Macromolecules 1997;30:2521–3.
[24] Shiotani T, Kobayashi G. Jpn Pat Appl; 1993:93049.
[25] Shimamura E, Kasuya K, Kobayashi G, Shiotani T, Shima Y, Doi Y. Macromolecules 1994;27:878–80.
[26] Doi Y, Kitamura S, Abe H. Macromolecules 1995;28:4822–8.
[27] Kichise T, Fukui T, Yoshida Y, Doi Y. Int J Biol Macromol 1999;25:69–77.
[28] Watanabe T, He Y, Fukuchi T, Inoue Y. Macromol Biosci 2001;1:75–83.
[29] Feng L, Watanabe T, Wang Y, Kichise T, Fukuchi T, Chen GQ, et al. Biomacromolecules 2002;3:1071–7.
[30] Yoshie N, Inoue Y. Int J Biol Macromol 1999;25:193–200.
[31] Feng L, Yoshie N, Asakawa N, Inoue Y. Macromol Biosci 2004;4:186–98.
[32] Yu F, Zhu B, Dong T, Inoue Y. Macromol Biosci 2009;9:702–12.
[33] Flory PJ. Principles of polymer chemistry. Ithaca, New York: Cornell University Press; 1953.
[34] Sato H, Nakamura M, Padrmshoke A, Yamaguchi H, Terauchi H, Ekgasit S, et al. Macromolecules 2004;37:7203–13.
[35] Avrami M. J Chem Phys 1939;8:212–24.
[36] Wunderlich B. Macromolecular physics, vol. 2. New York: Academic Press; 1976.